

The role of optimal vortex formation in biological fluid transport

John O. Dabiri* and Morteza Gharib

Graduate Aeronautical Laboratories and Bioengineering, California Institute of Technology, Pasadena, CA 91125, USA

Animal phyla that require macro-scale fluid transport for functioning have repeatedly and often independently converged on the use of jet flows. During flow initiation these jets form fluid vortex rings, which facilitate mass transfer by stationary pumps (e.g. cardiac chambers) and momentum transfer by mobile systems (e.g. jet-propelled swimmers). Previous research has shown that vortex rings generated in the laboratory can be optimized for efficiency or thrust, based on the jet length-to-diameter ratio (L/D), with peak performance occurring at $3.5 < L/D < 4.5$. Attempts to determine if biological jets achieve this optimization have been inconclusive, due to the inability to properly account for the diversity of jet kinematics found across animal phyla. We combine laboratory experiments, *in situ* observations and a framework that reduces the kinematics to a single parameter in order to quantitatively show that individual animal kinematics can be tuned in correlation with optimal vortex ring formation. This new approach identifies simple rules for effective fluid transport, facilitates comparative biological studies of jet flows across animal phyla irrespective of their specific functions and can be extended to unify theories of optimal jet-based and flapping-based vortex ring formation.

Keywords: vortex rings; fluid transport; cardiovascular flows; swimming; flying

1. INTRODUCTION

Jet flows in biological systems are typically created by the action of positive displacement pumps, which eject fluid from a source chamber through a nozzle or orifice (Vogel 1994). The flow regime of the jet can be characterized by the velocity of fluid exiting the chamber (U), the diameter of the jet at the chamber exit (D) and the kinematic viscosity of the fluid (ν). For Reynolds numbers $Re = UD/\nu > 6$, the period of rapid jet acceleration during flow initiation causes the leading portion of the jet to roll into a toroidal fluid mass known as a vortex ring (Cantwell 1986; see figure 1). Laboratory experiments have demonstrated that the leading vortex makes a proportionally larger contribution to mass and momentum transport than an equivalent straight jet of fluid (Krueger & Gharib 2003; Dabiri & Gharib 2004). This fact, along with the discovery that physical processes terminate growth of the leading vortex ring at a jet length-to-diameter ratio (L/D) between 3.5 and 4.5 (Gharib *et al.* 1998; Mohseni & Gharib 1998), has spurred interest in the possibility that biological systems may optimize vortex formation for effective fluid transport (Gharib *et al.* 1998; Linden & Turner 2001; Mohseni, Ran and Colonius 2001; Krueger & Gharib 2003; Dabiri & Gharib 2004; Linden & Turner 2004).

Inferences drawn from vortex rings generated in the laboratory are limited due to kinematic constraints on the vortex generators. Typically the vortices are created by ejecting fluid through a tube with constant exit diameter (Didden 1979; Gharib *et al.* 1998; Krueger & Gharib 2003; Dabiri & Gharib 2004). This is in contrast with the complex, time-dependant kinematics of positive displacement pumps found in nature (Vogel 1994). *In situ* measurements of fluid jet L/D (hereafter referred to as

the dimensionless ‘formation time’ following Gharib *et al.* 1998) have suffered from an inability to unambiguously incorporate the observed time-varying exit diameter $D(t)$. Attempts to reduce the observed kinematics using a time-averaged exit diameter (\bar{D}) have been inconclusive in determining a clear correlation between vortex formation dynamics and animal kinematics (Linden & Turner 2004; Anderson & Grosenbaugh 2005).

The average jet diameter is by itself an insufficient index of jet kinematics because it lacks critical information regarding temporal trends in the jet exit diameter. As mentioned above, laboratory experiments have pointed to the existence of a critical formation time, after which growth of the leading vortex ring ceases and any additional fluid ejected takes the form of a trailing straight jet (Gharib *et al.* 1998). Since this vortex-limiting formation time is dictated by the time-history of the jet exit diameter and not its average value, an effective kinematic index must preserve this information. From this we can properly record how jet flow is manipulated by changes in the exit diameter both before and after the vortex-limiting formation time is reached.

The goal of this paper is to combine laboratory experiments, *in situ* observations and a framework that reduces the kinematics to a single parameter in order to show that individual animal kinematics can be tuned in correlation with optimal vortex ring formation.

2. METHODS

(a) Kinematic analysis

A suitable kinematic parameter to describe observed animal motions can be derived by considering an infinitesimal increment in the formation time: $\Delta(L/D)^* \equiv (U(\tau)/D(\tau))\Delta\tau$, where $\Delta\tau$ is a small increment in dimensional time. Here, the jet exit velocity and diameter are instantaneous values at

* Author for correspondence (jodabiri@caltech.edu).

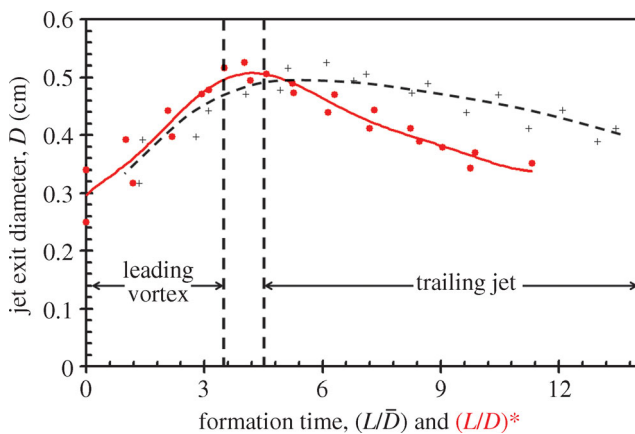


Figure 3. Tail-first swimming kinematics of *Lolliguncula brevis*. Jet exit diameter and velocity data from successive swimming cycles were compiled from Bartol *et al.* 2001. Dashed vertical lines indicate range of vortex-limiting formation time, $3.5 < (L/\bar{D})^* < 4.5$. Cross symbols indicate trends computed using L/\bar{D} as defined in the text. Circle symbols and solid line indicate trend computed using $(L/D)^*$ as defined in the text. Formation time calculations include the effect of background flow as in Krueger *et al.* (2003).

Where efficiency is secondary in importance to absolute thrust or impulse production, it will be useful to extend the duration of fluid ejection beyond the formation time of 4. Here, quasi-steady fluid dynamics can be exploited to further augment the thrust. For a given volume flow rate (\dot{Q}) ejected from the source pump after leading vortex ring growth has terminated, the exit flow velocity will be inversely proportional to the square of the exit diameter; $U \sim \dot{Q}/D^2$. Since the rate of fluid impulse production is proportional to U^2 (for a constant volume flow rate), decreasing the exit diameter after growth of the leading vortex ring has ceased will provide substantial gains in the jet flow's momentum transport.

In sum, animals that face selective pressures for efficiency will create flows with jet formation times approaching 4. Conversely, systems that require large thrust production—possibly at the expense of operational efficiency—will increase the exit diameter until a formation time of 4 is achieved, and then subsequently decrease the exit diameter for optimal performance during extended fluid ejection.

(c) Comparison with in situ squid measurements

We confirmed these predictions for two biological systems on opposite ends of the spectrum (functionally speaking) of biological jet flows. In the first case, we considered tail-first swimming of the brief squid *Lolliguncula brevis*. This mode of locomotion is employed by squid for high-speed manoeuvres, including their jet-propelled escape mechanism (Gosline & DeMont 1985; O'Dor 1988; Anderson & DeMont 2000; Bartol *et al.* 2001). A premium is accordingly placed on thrust production during this swimming mode. Following the foregoing discussion, the formation time should be larger than 4, with the squid funnel exit diameter temporally increasing until a temporal decrease occurs near the vortex-limiting formation time. Figure 3 plots data from published measurements of the time-dependent funnel exit diameter (i.e. $D(t)$) during successive swimming cycles (Bartol *et al.* 2001) versus jet formation times computed using the

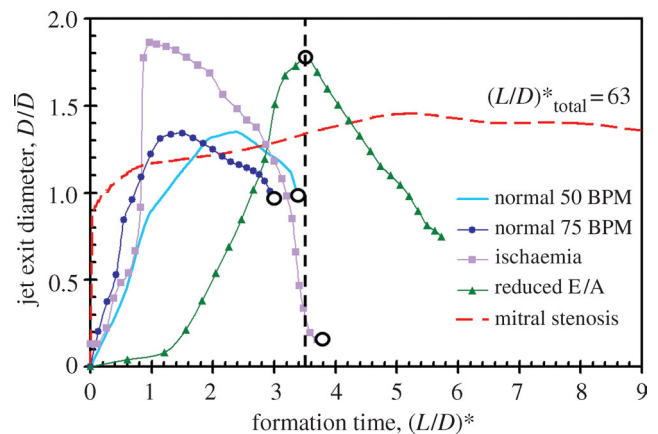


Figure 4. Transmittal flow during normal and pathological early diastolic filling (E-wave). Jet exit diameter and velocity data for each patient were compiled from Verdonck *et al.* (1996). Diameter data are normalized by the time-averaged mitral valve exit diameter in each patient to facilitate quantitative comparison. Dashed vertical line indicates lower bound of vortex-limiting formation time, $(L/D)^* = 3.5$. Open circle symbols indicate points of correlation with optimal vortex formation time.

methods presented above. When the funnel exit diameter is plotted versus the traditional formation time definition, that is, $D/(L/\bar{D})$ versus (L/\bar{D}) , there is no clear correlation between changes in the funnel exit diameter and the vortex-limiting formation time (crosses). However, using the parameter $(L/D)^*$ developed here, the exit diameter data $D((L/D)^*)$ is shifted to the left along the abscissa $(L/D)^*$ which leads to a sharper transition between initial funnel exit diameter increase and subsequent decrease (closed circles). Furthermore, the transition between the two phases follows the predicted behaviour, occurring in the range $3.5 < (L/D)^* < 4.5$.

(d) Comparison with in vivo cardiac measurements

As a second example, we examined published data from transmittal blood flow during early left ventricle diastolic filling in patients (Verdonck *et al.* 1996) measured using M-mode echocardiography (Nishimura *et al.* 1989). Figure 4 plots the mitral valve exit diameter versus jet formation time $(L/D)^*$ computed for normal and pathological conditions observed in patients.

During normal function (solid line), the entire jet is ejected in a formation time less than 4, indicating efficient operation. The initial rate of valve opening increases with heart rate (closed circles), providing the augmented fluid impulse required under the systemic stress. This observation is consistent with the relationship between fluid impulse and jet exit diameter noted in §3a. When the stresses are exacerbated, as in pathologies such as cardiac ischaemia (Gaasch & Zile 2004), a response is observed in the mitral valve kinematics in which the degree of temporal valve opening is increased (closed squares). Again, this is in accord with the principles we have outlined whereby such temporal increases in jet diameter provide increased impulse generation. Although this compensatory mechanism can be effective in the short term, further deterioration of the pump mechanism in the form of reduced performance at flow initiation (i.e. reduced E/A wave ratio; Appleton *et al.* 1988) can

force the system to abandon efficient function for the sake of merely producing sufficient fluid impulse to survive. In these cases, the jet formation time is increased beyond an $(L/D)^*$ approximate to 4 (closed triangles). Similar to the behaviour observed in the squid jet flows during high-speed and escape swimming, the resulting exit diameter kinematics follow our prediction of a temporally increasing exit diameter until the vortex-limiting formation time is reached, followed by temporal decrease thereafter.

Certainly, not all pathologies of left ventricle diastole can exploit these compensatory mechanisms. When the function of the valves themselves is affected, as in mitral valve stenosis (Gaasch & Zile 2004), any correlation between valve kinematics and the vortex-limiting formation time is lost (dashed line). However, this observation in itself serves as a useful diagnostic for pathologies that are localized near the jet exit plane.

4. DISCUSSION

This work has shown that functionally and morphologically diverse biological fluid transport systems can be designed and tuned using simple rules in accordance with the dynamics of vortex ring formation. The framework introduced here for studying biological jet flows has the potential to connect functionally disparate systems in comparative studies, and to improve our understanding of jet flow pathologies relative to normal function.

We also suggest that the analytical method developed here can be used to develop a connection between the observed robustness of jet-based vortex ring formation in aquatic propulsion (Linden & Turner 2004) and the previously discovered optimal Strouhal parameter for flapping-based vortex ring formation in insect and bird flight (Taylor *et al.* 2003). In an analysis of the latter group, the jet exit diameter of relevance in the present paper will be replaced with considerations for the time-dependent flap morphology and flapping kinematics.

We thank I. K. Bartol for kindly providing access to the *Loliguncula* data used in this work. This research is supported by National Science Foundation grant 0309671.

REFERENCES

- Anderson, E. J. & DeMont, M. E. 2000 The mechanics of locomotion in the squid *Loligo pealei*: locomotory function and unsteady hydrodynamics of the jet and intramantle pressure. *J. Exp. Biol.* **203**, 2851–2863.
- Anderson, E. J. & Grosenbaugh, M. A. 2005 Jet flow in steadily swimming adult squid. *J. Exp. Biol.* **208**, 1125–1146.
- Appleton, C. R., Hatle, L. K. & Popp, R. L. 1988 Relation of transmitral flow velocity patterns to left ventricular diastolic function: new insights from a combined hemodynamic and Doppler echocardiographic study. *J. Am. Coll. Cardiol.* **12**, 426–440.
- Bartol, I. K., Patterson, M. R. & Mann, R. 2001 Swimming mechanics and behaviour of the shallow-water brief squid *Loliguncula brevis*. *J. Exp. Biol.* **204**, 3655–3682.
- Cantwell, B. J. 1986 Viscous starting jets. *J. Fluid Mech.* **173**, 159–189.
- Dabiri, J. O. & Gharib, M. 2004 Fluid entrainment by isolated vortex rings. *J. Fluid Mech.* **511**, 311–331.
- Dabiri, J. O. & Gharib, M. In press. Starting flow through nozzles with temporally variable exit diameter. *J. Fluid Mech.*
- Didden, N. 1979 Formation of vortex rings—rolling-up and production of circulation. *Z. Angew. Math. Phys.* **30**, 101–116.
- Gaasch, W. H. & Zile, M. R. 2004 Left ventricular diastolic dysfunction and diastolic heart failure. *Annu. Rev. Med.* **55**, 373–394.
- Gharib, M., Rambod, E. & Shariff, K. 1998 A universal time scale for vortex ring formation. *J. Fluid Mech.* **360**, 121–140.
- Gosline, J. M. & DeMont, M. E. 1985 Jet-propelled swimming in squids. *Sci. Am.* **252**, 96–103.
- Krueger, P. S. & Gharib, M. 2003 The significance of vortex ring formation to the thrust and impulse of a starting jet. *Phys. Fluids* **15**, 1271–1281.
- Krueger, P. S., Dabiri, J. O. & Gharib, M. 2003 Vortex ring pinchoff in the presence of simultaneously initiated uniform background co-flow. *Phys. Fluids* **15**, L49–L52.
- Linden, P. F. & Turner, J. S. 2001 The formation of ‘optimal’ vortex rings, and the efficiency of propulsion devices. *J. Fluid Mech.* **427**, 61–72.
- Linden, P. F. & Turner, J. S. 2004 ‘Optimal’ vortex rings and aquatic propulsion mechanisms. *Proc. R. Soc. B* **271**, 647–653. (doi:10.1098/rspb.2003.2601.)
- Mohseni, K. & Gharib, M. 1998 A model for universal time scale of vortex ring formation. *Phys. Fluids* **10**, 2436–2438.
- Mohseni, K., Ran, H. Y. & Colonius, T. 2001 Numerical experiments on vortex ring formation. *J. Fluid Mech.* **430**, 267–282.
- Nishimura, R. A., Abel, M. D., Hatle, L. K. & Tajik, A. J. 1989 Assessment of diastolic function of the heart: background and current applications of Doppler echocardiography. Part 2: clinical studies. *Mayo Clin. Proc.* **64**, 181–204.
- O’Dor, R. K. 1988 The forces acting on swimming squid. *J. Exp. Biol.* **137**, 421–442.
- Shariff, K. & Leonard, A. 1992 Vortex rings. *Annu. Rev. Fluid Mech.* **24**, 235–279.
- Taylor, G. K., Nudds, R. L. & Thomas, A. L. R. 2003 Flying and swimming animals cruise at a Strouhal number tuned for high power efficiency. *Nature* **425**, 707–711.
- Verdonck, P., Segers, P., Missault, L. & Verhoeven, R. 1996 In vivo validation of a fluid dynamics model of mitral valve M-mode echocardiogram. *Med. Biol. Eng. Comput.* **34**, 192–198.
- Vogel, S. 1994 *Life in moving fluids*. Princeton: Princeton University Press.
- Willert, C. E. & Gharib, M. 1991 Digital particle image velocimetry. *Exp. Fluids* **10**, 181–193.